

Design Of A Chipless Rfid Tag Encoded In Polarization

O. Necibi, Ch. Guesmi, A. Gharsallah

Abstract: This paper focuses on the specific concepts of chipless Radio Frequency IDentification (RFID) tag destined for short range applications. The planar tag is composed of 3 nested Circular Split Ring Resonator (C-SRR) based on an angular encoding technique depend on polarization diversity. To validate the proposed approach, a tag with a coding capacity of 3 bits has been designed with a compact size of 6×6 mm². Tags with different orientation of an open ring have been simulated using a Rogers RO4003 substrate and their radar cross-section (RCS) responses have been presented. The proposed method is based on an angular encoding where its main advantage is to require a very reduced bandwidth compared to the Pulse Position Modulation (PPM) frequency coding techniques.

Index Terms: Radio Frequency Identification (RFID), Chipless RFID tags, encoding technique, data capacity, radio cross section (RCS), frequency response, resonance, polarization.

1. INTRODUCTION

Chipless RFID Tag is a relatively young discipline. We will see that the first published works date from 2002 and its potential application is undoubted. However, for technical reasons, there are today very few commercial applications based on its principle. In this context we are interested only in the development of chipless RFID whose information is encoded in the frequency domain. Indeed, with regard to the current state of the art, it has become clear that time coding techniques [1] [2] [3] [4] based on the use of low-permittivity substrate are still very far from reaching the surface coding densities of SAW tags [5] or frequency chipless tags [6] [7]. The reason is inherent in the used coding principle. Indeed, these tags encode the information according to the position of a pulse in time or its presence. To sufficiently separate two time positions so that the reflected signals do not overlap, it is necessary to add delay lines between each discontinuity. The smallest delay to be created depends on the pulse width of the emitted pulse. Thus for a pulse of 1 ns of width, a delay greater than 1 ns must be created to separate two reflections. To increase the number of time positions, it is therefore necessary either to increase the number of delay line sections or to reduce the width of the pulse. In both cases we run into the following problems:

- Increasing the number of line segments leads to a larger tag area. In addition, at each new discontinuity (at the origin of the reflection of a portion of the incident wave), the amplitude of the signal decreases which makes it doubly difficult to increase the length of the line.
- A very short pulse gives a spectral power density very spread in the frequency spectrum. However, decreasing the width of the pulse is not easy to achieve in practice. Moreover, it considerably increases the cost of the system for reading chipless tags. The maximum allowable unlicensed bandwidth specified by the FCC for ULB communications is between 3.1 and 10.6 GHz. What ultimately defines a pulse of minimum width of the order of a few tens of picoseconds. In addition, a filter output from the reader's pulse generator must be used to comply with the templates imposed by the standards on ULB

communications.

Teams working in this field have also sought to reduce the number of line sections and their sizes by combining a Quad phase-shift keying (QPSK) coding technique (thus improving the coding efficiency) with the use of Composite Right Left-Handed lines (CRLH) that can convey slow waves [1]. Unfortunately, this architecture remains too complex, and very delicate to realize. In addition, the necessary dimensions are imposing (20 cm long), all to encode 6 bits [1]. It is therefore absolutely not realistic from a practical point and non-competitive on the economic plan where the idea remains to be able to obtain tags with a unit cost lower than the euro cent. It is therefore logically that we are oriented towards the design of chipless tags encoded in the frequency domain. Indeed, in the literature, and contrary to time tags, coding capabilities of up to 35 bits on reduced surfaces were reported. Especially since unlike most time tag designs, the possibility of achieving the entire tag via low cost methods such as printing are quite possible with the proposed designs [7] [8] [9]. It seems to us that "frequency" tags have a much greater development potential than "time" tags. We can group tags using a frequency-coding approach into two large families. The first introduced by Preradovic et al. [7] uses a receiving antenna connected to a multi-band rejection filter. The second family uses a different concept that allows for potentially more compact structures. Indeed, the same type of electromagnetic response can be obtained with a structure using diffracting and filtering elements [8] [9] which integrate the 3 functions mentioned in the first family. That is, this compact element acts as both a receiving antenna, a filter, and a transmitting antenna.

At first sight, these diffracting elements could be assimilated to arbitrary radar targets. But to be more precise, it should be noted that the choice of this basic element must be made in such a way that it can generate a chosen and non-arbitrary electromagnetic signature. As a result, there must be a direct link between the encoding of an identifier and a particular geometry of the tag. Even if the very first designs introduced according to this principle have only weak coding capacity [7], it is interesting to compare the surface coding densities of each of these two technologies. Indeed, the size of the chipless tag is also an important element to take into consideration. The design of Jalaly et al. [9] offers a better density of surface coding with 0.8 bits / cm² against 0.6 bits / cm² for the solution of [7], the coding used in both cases being identical. This shows the miniaturization potential of this

• *Omrane Necibi, Jof university, College of Arts and Sciences at Tabrijal Computer science department Jof, Saudi arabia. E-mail: oncibi@ju.edu.sa*

approach. Our research work has therefore focused on the design of "frequency-free" chip tags based on the combination of diffracting elements. In most previous designs, the polarization aspect has not really been considered. Consequently, to detect the tag regardless of its orientation, the reader needs to change the polarization angle, which makes the reader more complex. In the following study [10] we present a tag based on the association of circular resonators. The main advantage of this form of resonator comes from the fact that their electromagnetic response is the same whatever the angle of polarization. This paper is organized as follows: Section 2 describes the Modeling of electromagnetic response. Section 3 introduces the design of the proposed antenna. This part will be concluded by introducing the results discussion and followed by conclusion in Section 4.

1 MODELING THE ELECTROMAGNETIC RESPONSE

Our developments will be based on the use of multiple filter reflectors. To better introduce this category of chipless tags, we will study the behavior of a reflector that can be seen as an object of any geometry, which has a conductive surface. It therefore reflects the electromagnetic waves in a particular and predictable way. This backscattered wave will be the signature of the tag. The principle here is to create resonance peaks, distinguishable from each other, in the chosen frequency spectrum. The phase change around resonances can also be used. To do this, it is necessary to use reflective elements with a very resonant behavior. Thus we will speak of resonators to designate filtering reflectors described here, that is to say based on a resonant behavior. From the electromagnetic response of a resonator it is possible to extract a model that makes it possible to make the connection between the geometry of the reflector and its identifier. From a practical standpoint, a model predicts the electromagnetic signature tags and therefore generate the corresponding geometries quickly without the need for heavy simulation. This precise point is rarely mentioned in the literature, it is no less important. Moreover, it should be noted that all the structures that we meet do not necessarily lend themselves to an analytical and deterministic modeling. We will see later; this model is different depending on whether a ground plane is used or not. Note that the decoding aspect (recovery of the identifier) is another problem that occurs regardless of the generation mode of the structure. It requires algorithms implementing signal processing functions. To begin, we'll talk about the basic element we've used to design different chipless tags. This element is the circular resonator with gap in the ring that we will call later for questions of facility resonator in C. This resonator can be seen as a dipole short-circuited in its center. More generally, a diffracting element can be considered as an antenna loaded by a complex impedance. The interest of this structure is its ability to resonate very selectively in frequency. Resonance occurs when one quarter of the wavelength of the incident signal is equivalent to the electrical length of the slot formed by the two arms of the circular resonator, thereby reducing the maximum resonator size by a factor of 2 compared to the dipole in short circuit. As we will see later, a polynomial analytical model can be extracted to connect the slot length to the resonant frequency. In addition, the combination of several resonators is possible in very small areas because the coupling between the elements is relatively limited. A transfer function (1) can be used to model the resonator. To do this we need to analyze

more precisely the electromagnetic response of the resonator in amplitude and phase. In the case of a resonator without a ground plane, we can observe around the resonance, for a zero incidence, a peak followed by a trough. The peak can be modeled by a pole of order 2. The hollow appears when two modes of resonance are in opposition of phase. Especially when there is a destructive interference between the low resonant structure mode and the very resonant antenna mode. Thus a C resonator can be modeled by the addition of two pass-band filters each having a second order pole as shown in FIG. 2 (a) and (b). To generalize this approach to the case of a tag without a multi-resonator chip, just add as many terms (1) as resonators.

$$T(\omega) = \frac{G_{struct} \cdot e^{-j\varphi_{struct}}}{1 + \frac{2m_{struct}j\omega}{\omega_{struct}} + \left[\frac{j\omega}{\omega_{struct}}\right]^2} + \frac{G_{res1} \cdot e^{-j\varphi_{res1}}}{1 + \frac{2m_1j\omega}{\omega_1} + \left[\frac{j\omega}{\omega_1}\right]^2} + \frac{G_{res2} \cdot e^{-j\varphi_{res2}}}{1 + \frac{2m_2j\omega}{\omega_2} + \left[\frac{j\omega}{\omega_2}\right]^2}$$

In equation (1), G_{struct} , G_{res1} and G_{res2} represent a gain term that characterizes the response level for, respectively, the structure mode and the first two resonant modes in the case where the tag has two resonators. The terms m_{struct} , m_1 and m_2 represent the damping coefficient and ω_{struct} , ω_2 , ω_3 are the resonance pulses of the modes already mentioned above. To complete each mode has a term characterizing a phase shift: $e^{-j\varphi_{struct}}$ for the mode structure and $e^{-j\varphi_1}$ and $e^{-j\varphi_2}$ for the first two resonant modes. It should be noted that this model does not take into account the higher order modes of the resonators (which do not participate in the coding and are beyond the detection system bandwidth) which intervene twice and three times resonance frequency of the first mode respectively for a half-wave and quarter-wave resonator.

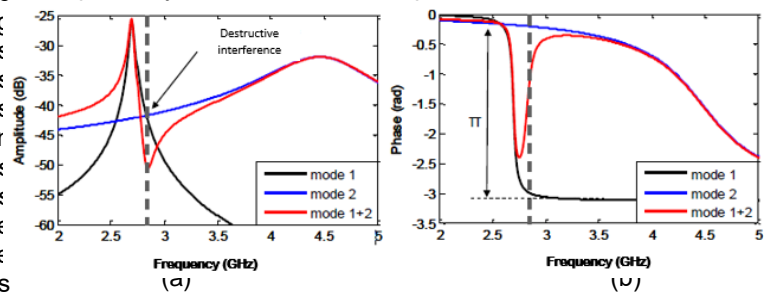


Figure 1. Illustration of the interference phenomenon using the expression (1), between the very resonant antenna mode (noted mode 1) and the mode of structure (noted mode 2) in the case of a resonator without a ground plane: (a) in amplitude, (b) in phase. The parameters of the

model with two resonance modes are: $f_{struct} = 2.7$ GHz, $f_1 = 4.5$ GHz, $G_{struct} = 0.005$, $G_1 = 0.001$, $m_{struct} = 0.1$ and $m_1 = 0.01$. Modes 1 and 2 are initially in phase therefore $\varphi_{struct} = \varphi_1 = 0$.

2 PRESENTATION OF DESIGN

The circular tags allow obtaining even unmatched performance in terms of polarization independence and coding capacity. We decided to use this feature to propose a new identification principle [11], based on an angular encoding where its main advantage is to require a very reduced bandwidth compared to the frequency PPM coding techniques. On the other hand, we also demonstrate that the

polarization sensitivity of the reflecting structures, allows for another type of use to realize an angle sensor in a variation range of 0° to 180°.

2.1 Description of the tag

Depending on the angle of polarization of the incident field, the electromagnetic response of an SRR resonator with ground plane, as shown in Fig. 2 (a), varies significantly.

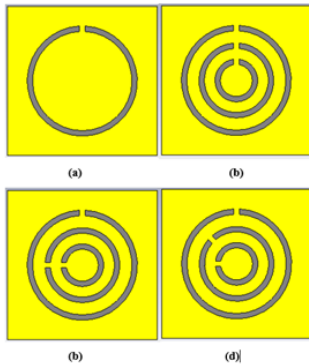


Figure 2. (a) Circular SRR resonator, (b), (c), and (d) Tag 1, 2 and 3 having 3 SRRs with various configurations.

It is therefore quite possible to encode an identifier according to the angle of polarization. For this, a more complex reader must be implemented implementing a polarization agility function. On the other hand, with this technique, it is possible to obtain tags having a large coding capacity while operating only in the ISM frequency bands. This is the main reason that motivated the study of this structure. The design shown in Fig. 2 (b) to (d) is based on the association of 3 nested circular SRR resonators. Depending on the position of the gap on the ring, the answer is not the same. The simulated electromagnetic response of a simple SRR resonator is shown in Fig. 3 for several angles of polarization ϕ .

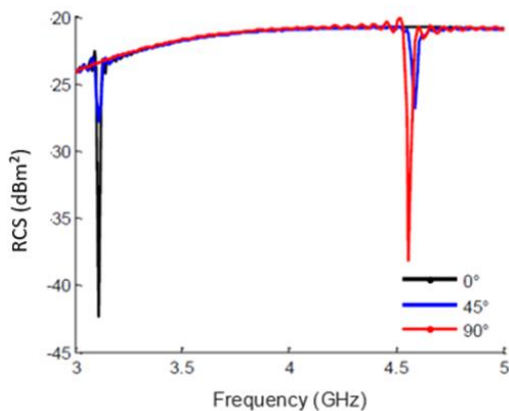


Figure 3. RCS of a circular SRR as a function of the frequency for several angles of polarization ϕ . The radius R of the SRR is 9.3 mm, the width w of the conductor 1 mm and the aperture g of 0.5 mm.

We note that for a polarization angle of 0° (vertical polarization), the interference dip at 3.1 GHz is clearly visible. The resonance mode is half-wavelength as in the case of a circular resonator without gap (see Fig. 4 (a)). For a 90° polarization angle (horizontal polarization), the resonance

mode is different. In this case, the first resonance occurs when the perimeter of the ring is equal to 3 times the half-wavelength, as shown in Fig. 4 (b). Fig. 2 shows a resonance frequency at 4.55 GHz; corresponding to an electrical length of $3\lambda / 2$ (the first mode in $\lambda / 2$ is no longer present). For intermediate angles (45°), we can see the two resonance frequencies appear with varying amplitudes. However, a strong contrast is visible between an angle of 0° and a 90° angle. In order to generate an identifier, we use two additional resonators as we can see Fig. 2 (b) to (d). Discrimination between the different resonators will again occur in frequency. Depending on the orientation of the tag with respect to the incident wave, and considering only the first resonance mode for each resonator, we can see three narrowband troughs in the spectrum. However, it should be noted that the second mode could be used to increase the robustness of decoding by providing some redundancy.

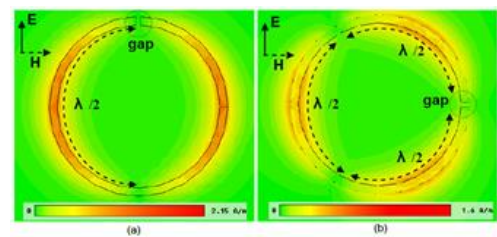


Figure 4. Surface current at resonance. (a) The gap is located at the top of the ring. The resonant frequency is 3.1 GHz. (b) The gap is located on one side of the ring. The resonance frequency is 4.5 GHz in this case. The resonator is excited by a plane wave in vertical polarization in both cases. The average radius of the circle is 9.3 mm, the track width is 1 mm and the width of the gap is 0.5 mm.

2.2 Coding principle

The coding technique used in this approach associates a specific identifier with an orientation of an open ring. In this way, a value '0' is assigned to it for a rotation angle of 0° (the reference here is the location of the gap), while the values '1', '2' and '3', will be assigned respectively for 45°, 90° and 135°. Thus, if we are interested only in the amplitude variation of the first resonance mode for each ring, a minimum indicates that the polarization angle of the wave corresponds to that of the ring (defined by the location of the gap). It should be noted that the angle of rotation of each resonator is considered relative to the angle of rotation of the resonator 1 (the largest), taken as a reference. Thus with the two resonators noted 2 and 3, we can code $4 \times 4 = 16$ identifiers as shown in the example shown in Fig. 4.

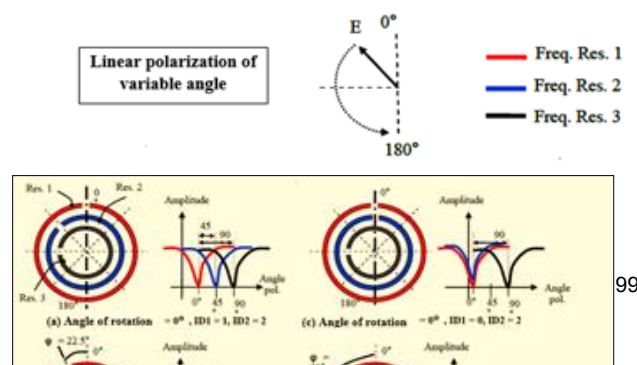


Figure 4. Description of the coding technique based on polarization diversity. (a) The tag is collinear with the incident wave ($\varphi = 0^\circ$, the reference for the orientation of the tag is the position of the gap of the resonator 1) and the resonators 2 and 3 are turned by $+45^\circ$ and $+90^\circ$ with respect to resonator 1. (b) The tag is rotated by $\varphi = 22.5^\circ$, resonators 2 and 3 are rotated by $+45^\circ$ and $+90^\circ$ always with respect to the resonator 1. (c) $\varphi = 0^\circ$, only the resonator 3 is rotated by $+90^\circ$. (d) $\varphi = 90^\circ$, and the resonators 2 and 3 are rotated 90° . For each configuration, a curve indicates the variation of the amplitude of the backscattered signal according to the polarization of the incident wave.

The ID1 is associated to the resonator 2, while ID2 is associated to the resonator 3. The first configuration illustrated in Fig. 5 (a) shows a tag having a rotation angle of 0° . In this tag, the resonator 2 has an angle of rotation $\alpha_1 = 45^\circ$ and the resonator 3 has an angle α_2 of 90° . Therefore, their identifier is ID1 = 1 and ID2 = 2, respectively. Regarding the case of Fig. 4 (b), from the reader's point of view, the tag is rotated at an angle of 22.5° . The 3 resonators are turned by 22.5° , however, the relative angles of the resonators 2 and 3 with respect to the resonator 1 remain unchanged, the identifier is not changed. The configurations illustrated in Fig. 5 (c) and (d) present two additional situations varying both the identifier of the tag and its angle of rotation. It should be noted that with this type of coding, even if the resonant frequencies vary slightly because of the presence of a disturbing environment, the identifier is not modified because it depends only on the geometry of the tag independently of the used substrate.

2.3 Results and discussions

To validate this coding principle, the three tags shown in Fig. 2 (b) to (d) were simulated. The substrate used is Roger RO4003 having a thickness of 0.5 mm. The radius of the circles is identical for the 3 tags and are respectively 8.56 mm, 5.55 mm and 4.11 mm for the resonators noted 1 to 3. The resonance frequencies associated for the first modes are respectively 3.4 GHz, 5.25 GHz and 7.07 GHz. The position of the gaps varies from one tag to another. In the tag 1, the resonators 2 and 3 are turned respectively by 45° and 90° relative to the resonator 1. In the tag 2, the resonators 2 and 3 are not rotated relative to the resonator 1 while in the tag 3, they are turned 90° .

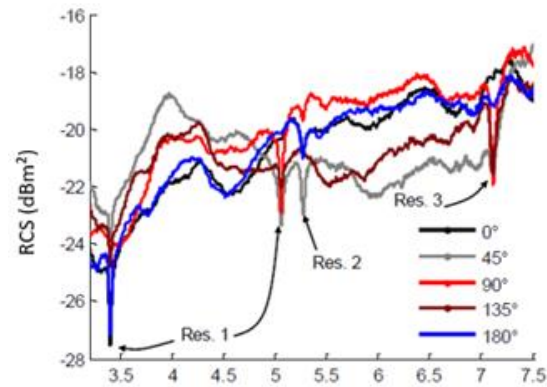


Figure 5. Simulated response of tag 1 in amplitude: (a) over the entire band.

For the coding of information, the extreme positions between 0° and 90° are used because they generate the greatest contrast at the level of the reflected amplitude.

Using equation (2) it is possible to determine the maximum number of combinations for this tag.

$$N = \lceil 18.0 / \Delta\varphi \rceil k$$

(2)

In this equation, N is the number of combinations, k is the number of resonators participating in the coding and $\Delta\varphi$ is the angular resolution. The value 180 corresponds to the maximum variation range of the polarization angle, since the information obtained according to this parameter is redundant every 180° . Using (2), we can find a coding capacity of $9 \times 9 = 81$ combinations, or 6.34 bits. The simulations carried out confirm the pronounced sensitivity of these resonators to polarization. At the level of the detection system, it is conceivable to make a reader operating in the ISM frequency bands. It suffices, for example, to modify the dimensions of the resonators so that they resonate in the band 860-960 MHz for the first, 2.45 GHz for the second and 5.8 GHz for the latter. In an identification application, the tag does not rotate, so it is at the reader that you must be able to orient the polarization of the interrogation signal to extract the identifier of the remote tag. Antennas implementing polarization diversity must be developed for this task.

3 CONCLUSION

An ultra-low cost, printable and compact chipless RFID Tag has been presented. Here, one major advancement in chipless RFID tag development are shown which is an angular encoding technique based on polarization diversity to increase overall data capacity.

ACKNOWLEDGMENT

The authors wish to thank University of Tunis El Manar, Faculty of Sciences of Tunis and Jouf university, Saudi arabia.

REFERENCES

- [1] MANDEL C, SCHUSSLER M, MAASCH M & JAKOBY R. A novel passive phase modulator based on lh delay lines for chipless microwave rfid applications. Wireless Sensing, Local Positioning, and RFID, 2009. IMWS 2009. IEEE MTT-S International Microwave Workshop on, 2009, p.1-4.

- [2] VEMAGIRI J, CHAMARTI A, AGARWAL M & VARAHRAMYAN K. Transmission line delay- π based radio frequency identification (rfid) tag. *Microwave and optical technology letters*, 2007, vol. 49, p.1900-1904.
- [3] ZHANG L, RODRIGUEZ S, TENHUNEN H & ZHENG L. An innovative fully printable rfid technology based on high speed time-domain reflections. *High Density Microsystem Design and Packaging and Component Failure Analysis*, 2006. HDP'06. Conference on, 2006, p.166-170.
- [4] ZHENG L, RODRIGUEZ S, ZHANG L, SHAO B & ZHENG L. Design and implementation of a fully reconfigurable chipless rfid tag using inkjet printing technology. *Circuits and Systems*, 2008. ISCAS 2008. IEEE International Symposium on, 2008, p.1524- 1527.
- [5] HARTMANN C. A global saw id tag with large data capacity. *Ultrasonics Symposium*, 2002. Proceedings. 2002 IEEE, 2002, p.65-69.
- [6] PRERADOVIC S, ROY S & KARMAKAR N. Fully printable multi-bit chipless rfid transponder on flexible laminate. *Microwave Conference*, 2009. APMC 2009. Asia Pacific, 2009, p.2371-2374.
- [7] PRERADOVIC S & KARMAKAR N. Design of fully printable planar chipless rfid transponder with 35-bit data capacity. *Microwave Conference*, 2009. EuMC 2009. European, 2009, p.13-16.
- [8] MCVAY J, HOORFAR A & ENGHETA N. Theory and experiments on peano and hilbert curve rfid tags. *Proceedings of SPIE*, 2006, p.624808.
- [9] JALALY I & ROBERTSON I. Rf barcodes using multiple frequency bands. *Microwave Symposium Digest*, 2005 IEEE MTT-S International, 2005, p.1-4.
- [10] VENA A, PERRET E & TEDJINI S. High capacity chipless rfid tag insensitive to the polarization. *IEEE Transactions on Antennas and Propagation*, 2012, p.1-7.
- [11] A. Vena, E. Perret, and S. Tedjini, "Chipless RFID Tag Using Hybrid Coding Technique," *IEEE Transactions on Microwave Theory and Techniques*, vol. 59, 2011.